Accepted Manuscript

Synthesis and application of near-infrared absorbing morpholino-containing aza-BODIPYs

Xin-Dong Jiang, Lei Jia, Yajun Su, Chen Li, Changliang Sun, Linjiu Xiao

PII: S0040-4020(19)30718-5

DOI: https://doi.org/10.1016/j.tet.2019.06.046

Reference: TET 30438

To appear in: *Tetrahedron*

Received Date: 1 May 2019

Revised Date: 26 June 2019

Accepted Date: 28 June 2019

Please cite this article as: Jiang X-D, Jia L, Su Y, Li C, Sun C, Xiao L, Synthesis and application of near-infrared absorbing morpholino-containing aza-BODIPYs, *Tetrahedron* (2019), doi: https://doi.org/10.1016/j.tet.2019.06.046.

Synthesis and application of near-infrared absorbing morpholino-containing aza-BODIPYs

Xin-Dong Jiang*[,a,b], Lei Jia[a], Yajun Su[a], Chen Li[a], Changliang Sun[a], Linjiu Xiao[a]

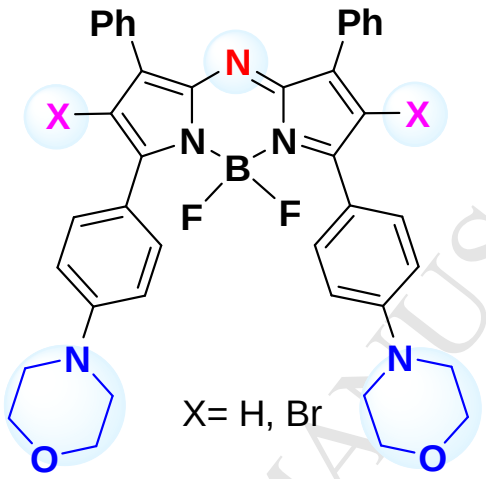

Graphical Abstract

Synthesis and application of near-infrared absorbing morpholino-containing aza-BODIPYs

Leave this area blank for abstract info.

Xin-Dong Jiang[*,a,b] , Lei Jia[a], Yajun Su[a], Chen Li[a], Changliang Sun[a], Linjiu Xiao[a]*

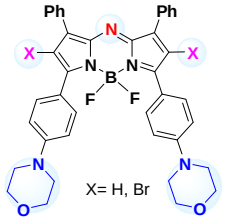

ELSEVIER

Tetrahedron

journal homepage: www.elsevier.com

Synthesis and application of near-infrared absorbing morpholino-containing aza-BODIPYs

Xin-Dong Jiang*[,a,b1], Lei Jia[a], Yajun Su[a], Chen Li[a], Changliang Sun[a], Linjiu Xiao[a]

[a]*College of Applied Chemistry, Shenyang University of Chemical Technology, Shenyang 110142, China*
[b]*Department of Chemistry, Graduate School of Science, Hiroshima University, 1-3-1 Kagamiyama, Higashi-Hiroshima 739-8526, Japan.*

ARTICLE INFO

Article history:
Received
Received in revised form
Accepted
Available online

Keywords:
Aza-BODIPY
Near-infrared
Morpholino
pH
PS

ABSTRACT

Morpholino-containing aza-BODIPYs at 3,5-positions were synthesized. The maxima absorption and emission of these dyes locate at the near-infrared region. Aza-BODIPY **1** with the morpholino group as a pH-sensitive functionality could be used to be a pH probe, and the dramatic increase in fluorescence intensity at 675 nm by about 1500 folds. Moreover, the singlet oxygen generation of PS **2** with the dibromo groups at 2,6-positions was more effective than that of the parent dye **1**.

1. Introduction

Since near-infrared (NIR) fluorescent dyes can greatly reduce background absorption, fluorescence and light scattering, and improve the sensitivity of fluorescent probe, NIR absorbing dyes are widespreadly applicable, such as molecular imaging, theranostics, photodynamic therapy, laser generators, electroluminescent devices, construction of light emitting diodes (OLED) and photovoltaic cells and so forth [1-3]. By employing borondipyrromethene (BODIPY) and aza-borondipyrromethene (aza-BODIPY) dyes the desired functionalization could be achieved [4-13]. Aza-BODIPY with a nitrogen atom at the meso-position in the dipyrromethene ligand is a promising candidate for NIR-absorbing dye because of their intrinsic narrow band gaps [14-18]. Moreover, by modifying the core of aza-BODIPYs, their derivatives, such as conformationally restricted aza-BODIPYs, heteroaryl-fused aza-BODIPYs, have been developed to extend the emission wavelength covering the NIR region (> 650 nm) [19-24]. Therefore, design of aza-BODIPYs has been attracting increasing interest.

It is known that, by introducing an electron-donating group one can further reduce the HOMO-LUMO gap by increasing the HOMO and/or decreasing the LUMO energy and reach bathochromic absorption and emission bands [25-30]. Apart from a few studies on aza-BODIPYs with an electron-donating group such as -(*p*-NMe_2)Ph/-(*p*-OMe)Ph at 3,5-positions [31], to the best of our knowledge, no aza-BODIPY with morpholino group at 3,5-positions has been documented. Additionally, introduction of the morpholine moiety as a recognition unit could be a latent application for monitoring pH value or lysosomal viscosity [32]. And, the pH probe for strong acid is adapted to study acidic organelles such as gastric acid, lysosomes and endosomes.[33] Additionally, it was noted that introducing an electron donating group (such as $–NMe_2$) resulted in the photosensitizer (PS) with higher singlet oxygen quatumn yield [34]. Our recent research interest lies in the novel aza-BODIPY family of fluorescent dyes [35-40]. We are interested in the influence of the morpholino groups at 3,5-positions on the properties of aza-BODIPY dyes. So, herein we report the synthesis of aza-BODIPYs **1** and **2** with the morpholino group at 3,5-positions, and their application for a pH probe and a PS (Fig. 1).

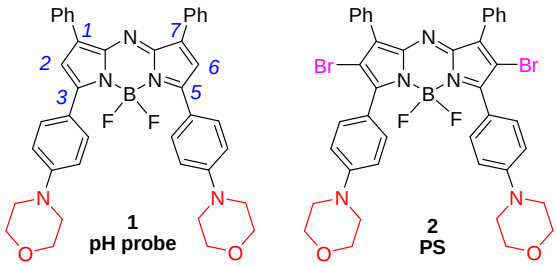

Fig. 1. Design strategy for aza-BODIPYs with the morpholino groups at 3,5-positions.

2. Result and discussion

One-step synthesis of pyrrole **4** was obtained by reaction of 1-(4-morpholinophenyl)ethanone **3** with 3-phenyl-2*H*-azirine in presence of NaH (Scheme 1) [41]. Then, the morpholino-containing pyrrole **4** was found to yield the symmetric aza-BODIPY **1** in the presence of HOAc, Ac_2O and $NaNO_2$, followed

* 1 Corresponding author. Tel.: +86 024 89387219.
E-mail address: xdjiang@syuct.edu.cn (X.-D. Jiang).

by complexation with $Et_3N–BF_3·Et_2O$ (Scheme 1) [42]. Aza-BODIPY **1** reacted with *N*-bromosuccinimide (NBS) to produce the dibromo-substituted aza-BODIPY **2** (Scheme 1). Dye **1** showed two sets of distinct hydrogen signals for the morpholine rings in the ^1H NMR spectrum (δ = 3.86 (t, $^3J_{HH}$ = 5.0 Hz, 8H) and 3.33 (t, $^3J_{HH}$ = 5.0 Hz, 8H) ppm), which is in agreement with those of the reported dyes [43,44].

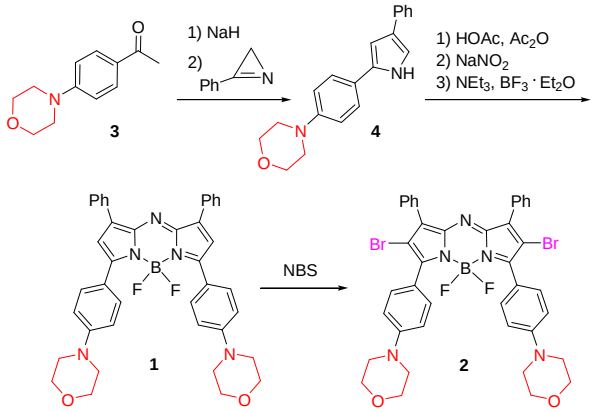

Scheme 1. Synthesis of NIR-absorbing morpholino-containing aza-BODIPYs at 3,5-positions.

The spectra of absorption and fluorescence of aza-BODIPYs **1** and **2** are outlined and shown in Fig. 2 and Table 1. Obviously, the maxima absorption and emission of **1** and **2** ($\lambda_{abs}/\lambda_{em}$ = 764/828 nm for **1**, 746/821 nm for **2**) locate at the NIR region. Aza-BODIPYs **1** and **2** have the high extinction coefficients. The full width half maximum (Fwhm = 128 nm) of **2** was broader than that (100 nm) of dye **1**. Owing to the intramolecular charge transfer (ICT) effect [45,46] by the introduction of the morpholine ring, the fluorescent quantum yield of aza-BODIPY **1** is low and dibromo-substituted aza-BODIPY **2** is nearly not fluorescent. In addition, the spectral qualities of the morpholino-containing aza-BODIPYs are comparable to those of dimetylamino-containing aza-BODIPYs [22].

Table 1. Photophysical properties of aza-BODIPYs **1** and **2** in CH_2Cl_2 at 293 K.

Dye	$\lambda_{abs}/\lambda_{em}$ [nm]	FWHM[nm]	ε [M^{-1} cm^{-1}]	Φ_f
1	764/828	100	86000	0.02
2	746/821	128	79000	NA

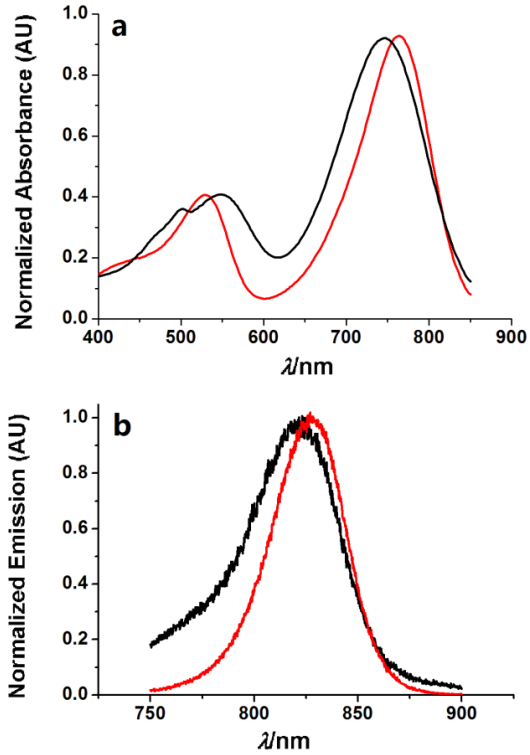

Fig. 2. (a) Normalized absorption and (b) fluorescence spectra of 2 μM **1** (black) and 2 μM **2** (red) in CH_2Cl_2 at 293 K. λ_{ex} = 730 nm.

The most popular strategy for pH-responsive fluorescent probe employs ICT or PET. The excited state of the fluorophore can be quenched by the electron transfer from electron donating amine to the fluorophore. Upon recognition of a proton, the electron transfer is “switched off” and in turn the emission of fluorescence is “switched on”. Therefore, morpholino group could be used for this purpose of ICT/PET. So, we continue to explore the response of the morpholino-containing aza-BODIPY **1** to pH value. For most biological applications a good water solubility is essential. For example, a fluorescent probe should be water soluble for effective detection of the analyte in live cells. However, it is unfortunate that sensing experiment in water were not successful due to poor water solubility of dye **1**. So, the mixture solution of CH_3CN/H_2O (9:1, v/v) was herein used. Photo image of **1** were taken under normal room illumination, and notable changes of relatively vivid bright colors of **1** with the pH (pH 7–12 M) can be easily observed with naked eye (Fig. 3). Upon addition of hydrochloric acid to aza-BODIPY **1** with the morpholino group as a pH-sensitive functionality, **1** could be protonated at the limitative pH value. A stepwise decrease of the absorption intensity was observed in the 800 nm band (Fig. 4). Then, the formation of a new band for **1**-$\mathbf{H}^+$ at 750 nm was observed in 2 M, and another new peak for **1**-2$\mathbf{H}^+$ subsequently arose at 647 nm in 12 M (Fig. 4 and 5). The absorption band of **1**-2$\mathbf{H}^+$ is blue-shifted by about 153 nm compared to that of **1**. The fluorescence of **1** in CH_3CN/H_2O (9:1, v/v) is quenched due to the ICT effect. The reversibility of the probe **1** between pH 7.0 and 2 M was also studied. The results showed that the process is reversible for at least six cycles (Fig. S2). Additionally, the detection limit to hydrochloric acid was calculated to be pH 4.2 (3σ/slope, Fig. S3). With decreasing pH the emission maxima were shifted to 675 nm (Fig. 6). A dramatic increase in fluorescence intensity at 675 nm by about 1500 folds (Φ_f = 0.37 when treated with HCl to 12 M)

(Fig. 6).

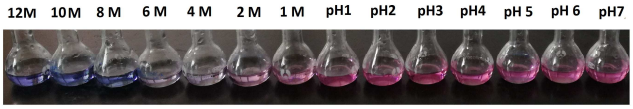

Fig. 3. Photographs of solutions of 4 μM dye **1** at pH 7, 6, 5, 4, 3, 2, 1 and 1 M, 2 M, 4 M, 6 M, 8 M, 10 M, 12M of HCl in CH_3CN/H_2O (9:1, v/v) under normal room illumination.

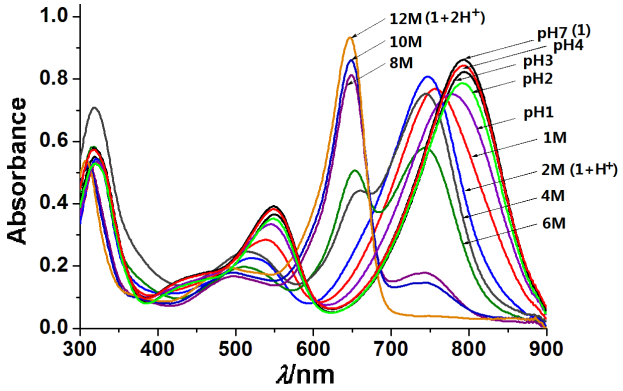

Fig. 4. Absorption spectra (pH 7, 6, 5, 4, 3, 2, 1 and 1 M, 2 M, 4 M, 6 M, 8 M, 10 M, 12M of HCl) of 4 μM dye **1** in CH_3CN/H_2O (9:1, v/v) as a function of pH.

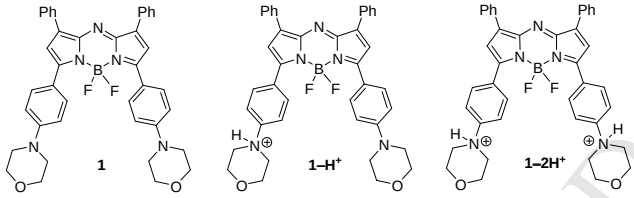

Fig. 5. Structures of dye **1**, protonated dyes **1-H**$^+$ and **1-2H**$^+$.

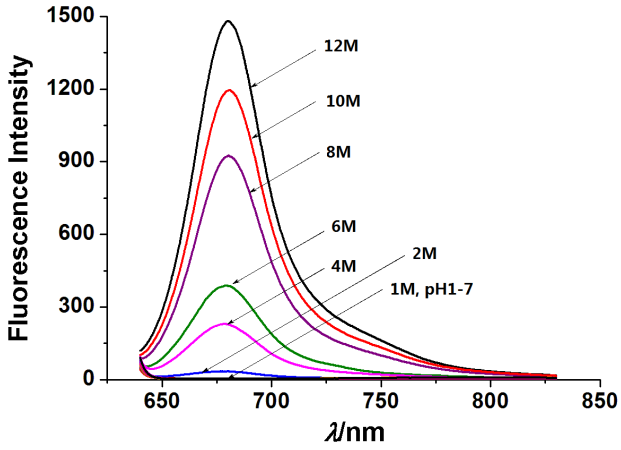

Fig. 6. Corresponding fluorescence spectra (pH 7, 6, 5, 4, 3, 2, 1 and 1 M, 2 M, 4 M, 6 M, 8 M, 10 M, 12M of HCl, λ_{ex} = 630 nm) of 4 μM dye **1** in CH_3CN/H_2O (9:1, v/v) as a function of pH.

Moreover, the molecular geometries of aza-BODIPY **1**, **1-H**$^+$ and **1-2H**$^+$ were optimized using density functional theory (DFT) at the B3LYP/6-31G(d) level [47]. The protonation of aza-BODIPY (**1-H**$^+$: λ_{abs} = 750 nm; **1-2H**$^+$: λ_{abs} = 647 nm) showed a remarkable hypsochromic shifts compared to that (λ_{abs} = 800 nm) of the aza-BODIPY **1**. It is due to the increase in the HOMO–LUMO band gap (2.03 ev; 1.99 ev) for the lowest energy absorption bands of **1-H**$^+$ and **1-2H**$^+$ relative to that (1.94 ev) of **1** by MO calculations (Fig. 7).

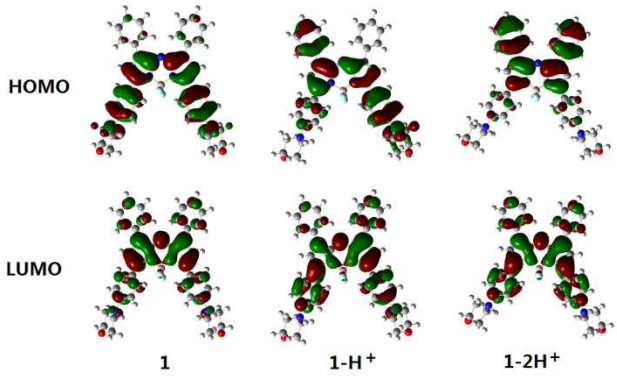

Fig. 7. Frontier molecular orbitals of aza-BODIPYs **1**, **1-H**$^+$ and **1-2H**$^+$ at the B3LYP/6-31G(d) level with Gaussian 09. HOMO/ LUMO (eV) = –4.81/–2.87 for **1**; HOMO/ LUMO (eV) = –6.98/–4.99 for **1-H**$^+$; HOMO/ LUMO (eV) = –9.23/–7.29 for **1-2H**$^+$.

Then, investigation of the singlet oxygen generation was performed to assess the ability of dibromo-substituted aza-BODIPYs **1** and **2** as the PS in toluene. To simulate a deep tissue penetration and to reduce the normal cell-damage, the NIR monochromatic light at 730 nm by using a 150 W xenon lamp at 0.5 mW/cm^2 was selected to irradiate the toluene solution [48]. 1,3-Diphenylisobenzofuran (DPBF) as a singlet oxygen indicator was employed to estimate singlet oxygen generation. The initial concentrations of 6.5 × 10^{-6} M of dyes **1** and **2**, and 6 × 10^{-5} M of DPBF was performed in this experiment. When the oxidation of DPBF with the generated singlet oxygen was carried out, the absorption maximum of DPBF at 416 nm was found to be gradually decreased. It is well-known that the singlet oxygen generation from a PS is regulated by the efficiency of a spin-forbidden electronic transition from a singlet to a triplet state upon irradiation [34]. The heavy atom effect is advocated to improve intersystem crossing (ISC) and consequently to generate the singlet oxygen. Therefore, the experimental results indicated that the singlet oxygen generation of PS **2** with the dibromo groups at 2,6-positions (Fig. 8 and 9) was more effective than that of **1**. A 3-fold rate enhancement is observed for **2** compared to **1** (Fig. 9 and Fig. S1). And, no photobleaching of **2** was found during this experiment, based on the absorption intensity (λ_{abs} = 755 nm in toluene) (Fig. 8). These results indicated that the NIR-absorbing PS **2** was able to be used for the generation of the singlet oxygen [49, 50].

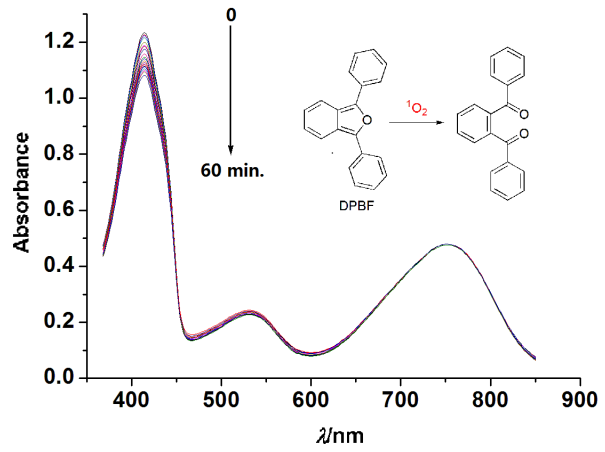

Fig. 8. DPBF (initial concentration at 6 × 10^{-5} M) degradation profile in toluene by dye **2** (6.5 × 10^{-6} M). Monochromatic light (730 nm at 0.5 mW/cm^2) used. The curves display time-dependent decrease (0, 3, 6, 9, 12, 15, 18, 21, 24, 27, 30, 33, 36, 39, 42, 45, 48, 51, 54, 57 and 60 min.) of absorbance at 416 nm by oxidation of DPBF with dye **2**.

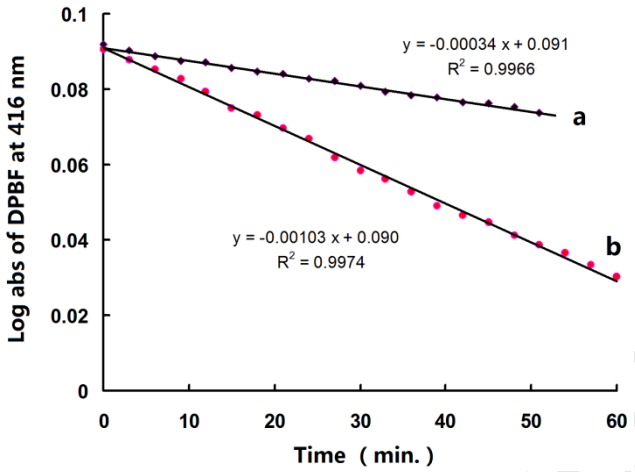

Fig. 9. Time-dependent decrease (0, 3, 6, 9, 12, 15, 18, 21, 24, 27, 30, 33, 36, 39, 42, 45, 48, 51, 54, 57 and 60 min.) of Log absorbance at 416 nm by oxidation of DPBF with **1** (*a* line) and **2** (*b* line).

3. Conclusions

In conclusions, aza-BODIPYs with the morpholino group at 3,5-positions were prepared. Aza-BODIPY **1** ($\lambda_{abs}/\lambda_{em}$ = 764/828 nm) and dibromo-substituted aza-BODIPY **2** ($\lambda_{abs}/\lambda_{em}$ = 746/821 nm) are the NIR-absorbing dyes. Due to the introduction of the morpholine ring lead to the ICT effect, the fluorescent quantum yield of aza-BODIPY **1** is low and dibromo-substituted aza-BODIPY **2** is not fluorescent. Upon addition of hydrochloric acid to aza-BODIPY **1** with the morpholino group as a pH-sensitive functionality, the formation of a new band for **1**-**H**$^+$ at 750 nm was observed in 2 M, and another new peak for **1**-2**H**$^+$ subsequently arose at 647 nm in 12 M. A dramatic increase in fluorescence intensity at 675 nm by about 1500 folds (Φ_f = 0.37 when treated with HCl to 12 M). The singlet oxygen generation of PS **2** with the dibromo groups at 2,6-positions was more effective than that of the parent dye **1**, and no photobleaching of **2** was found, indicating that the NIR-absorbing PS **2** was able to be used for the generation of the singlet oxygen.

4. Experimental section

4.1. General remarks

All reactions utilizing air- or moisture-sensitive reagents were performed in dried glassware under an atmosphere of dry N_2. ^{1}H NMR spectra were recorded on a VARIAN Mercury 500 MHz spectrometer at 20 ºC. ^{1}H NMR chemical shifts (δ) are given in ppm downfield from Me_4Si, determined by residual chloroform (δ = 7.26 ppm). ^{13}C NMR spectra were recorded on a VARIAN Mercury 125 MHz spectrometer at 20 ºC, and all signals are reported in ppm with the internal chloroform signal at δ 77.0 ppm as standard. Fluorescence spectra were recorded on an F-280 spectrophotometer at room temperature and are reported as cm^{-1}. UV/Vis spectra were recorded on a UV-2550 spectrophotometer at room temperature. All pH measurements were performed with a PHS-3E pH meter. The refractive index of the medium was measured by 2 W Abbe's refractometer at 20 °C.

The fluorescence quantum yields (Φ_f) of the aza-BODIPY systems were calculated using the following relationship (equation 1):

$$\Phi_f = \Phi_{ref} F_{sampl} A_{ref} n^2_{sampl} / F_{ref} A_{sampl} n^2_{ref} \quad (1)$$

Here, *F* denotes the integral of the corrected fluorescence spectrum, *A* is the absorbance at the excitation wavelength, and *n* is the refractive index of the medium, *ref* and *sampl* denote parameters from the reference and unknown experimental samples, respectively.

The reference systems used were boronazadipyrromethene compound aza-BODIPY (Φ_f = 0.36 in chloroform) [50] as standard for **1** and **2**.

The MO calculations were performed at the DFT level, and the frontier molecular orbitals of BODIPY **1**, **1**-**H**$^+$ and **1**-2**H**$^+$ at the B3LYP/6-31G(d) level with Gaussian 09 [47].

4.2. Synthesis

*4.2.1 Synthesis of pyrrole **4***

Under N_2, 1-(4-morpholinophenyl)ethanone **3** (300.0 mg, 1.46 mmol) was added to NaH (70.1 mg, 1.75 mmol) in DMSO (15 ml) at 25 °C and stirred for 10 min. Then, 3-phenyl-2*H*-azirine (173 mg, 1.47 mmol) was added and the resulting mixture was stirred for 3 h at the same temperature. It was quenched with water, neutralized with dilute HCl to a pH about 7. The mixture was extracted with CH_2Cl_2 (2 × 40 ml), and the organic layer was washed with brine (2 × 40 ml) and dried over anhydrous $MgSO_4$. After removal of the solvents by evaporation, the resulting crude mixture was separated by column chromatography (*n*-hexane : CH_2Cl_2 = 1 : 4) to afford **4** as green solids (155.4 mg, 35%). ^{1}H NMR (500 MHz, $CDCl_3$): δ (ppm) 8.41 (br s, 1H), 7.47 (d, ^3J = 9.0 Hz, 2H), 7.44 (d, ^3J = 7.5 Hz, 2H), 7.38 (s, 1H), 7.37 (s, 1H), 7.38 (t, ^3J = 7.5 Hz, 2H), 7.18 (t, ^3J = 7.5 Hz, 1H), 6.81 (d, ^3J = 9.0 Hz, 2H), 3.23 (t, ^3J = 4.5 Hz, 4H), 3.18 (t, ^3J = 4.5 Hz, 4H). ^{13}C NMR (125 MHz, $CDCl_3$): δ (ppm) 154.2, 131.3, 130.3, 129.7, 129.4, 128.5, 128.1, 125.1, 124.9, 116.0, 114.1, 113.2, 66.5, 47.5. HRMS-MALDI (m/z): [M+H]$^+$ calcd for $C_{20}H_{21}N_2O$: 305.1648, found 305.1651.

*4.2.2 Synthesis of aza-BODIPY **1***

Sodium nitrite (16.9 mg, 0.24 mmol) was added to a suspension of pyrrole **4** (150 mg, 0.49 mmol) in a mixture of acetic acid/anhydride (2 ml/0.8 ml) at room temperature. After 1 h stirring at room temperature, crushed ice was added to the mixture. The resulted dark green dye was filtered, washed with

water. The dark green dye was dissolved in CH_2Cl_2, filtered through a pad of alumina (activity III). Solvent was removed under reduced pressure, and the residue was dissolved in dry CH_2Cl_2. Triethylamine (0.10 ml, 0.71 mmol) was added, followed by dropwise addition of $BF_3{\cdot}Et_2O$ (0.13 ml, 1.05 mmol) with stirring at room temperature. The mixture was stirred for 2 h at room temperature. The reaction was quenched with crushed ice, extracted with CH_2Cl_2. The resulting crude mixture was separated by column chromatography on silica gel (*n*-hexane : CH_2Cl_2 = 1 : 3), and followed by recrystallization from CH_2Cl_2/*n*-hexane to afford **1** (67.2 mg, 42%) as coppery solids. ^{1}H NMR (500 MHz, $CDCl_3$): δ (ppm) 8.11 (d, ^3J = 8.5 Hz, 4H), 8.07 (d, ^3J = 8.5 Hz, 4H), 7.45 (t, ^3J = 7.0 Hz, 4H), 7.39 (t, ^3J = 7.0 Hz, 2H), 7.07 (s, 2H), 7.45 (d, ^3J = 8.5 Hz, 4H), 3.86 (t, ^3J = 5.0 Hz, 8H), 3.33 (t, ^3J = 5.0 Hz, 8H). ^{13}C NMR (125 MHz, $CDCl_3$): δ (ppm) 156.8, 152.3, 145.2, 141.8, 132.7, 131.5, 129.8, 129.1, 128.4, 121.8, 118.3, 113.9, 66.5, 47.4. HRMS (ESI) m/z calcd for $C_{40}H_{37}BF_2N_5O_2^+$ $(M+H)^+$ 668.30029, found 668.30048.

4.2.3 Synthesis of aza-BODIPY 2

Aza-BODIPY **1** (46.1 mg, 0.069 mmol) was treated with N-bromosuccinimide (143 mg, 0.801 mmol) in dry CCl_4 (20 ml) at 80 °C under nitrogen for 5 h. The reaction was quenched with water, extracted with CH_2Cl_2, and purified by chromatography on silica gel followed by recrystallization from CH_2Cl_2/*n*-hexane to afford **2** (40.3 mg, 71%) as dark coppery solids. ^{1}H NMR (500 MHz, $CDCl_3$): δ (ppm) 7.85 (d, ^3J = 7.0 Hz, 4H), 7.81 (d, ^3J = 8.5 Hz, 4H), 7.41-7.46 (m, 6H), 6.93 (d, ^3J = 8.5 Hz, 4H), 3.85 (t, ^3J = 5.0 Hz, 8H), 3.32 (t, ^3J = 5.0 Hz, 8H). ^{13}C NMR (125 MHz, $CDCl_3$): δ (ppm) 154.9, 147.7, 142.1, 134.3, 132.5, 130.9, 128.8, 127.8, 125.4, 119.3, 117.1, 113.1, 65.5, 47.4. HRMS (ESI) m/z calcd for $C_{40}H_{35}BBr_2F_2N_5O_2^+$ $(M+H)^+$ 826.11927, found 826.11920.

5. Acknowledgements

This work was supported by the National Natural Science Foundation of China (21542004), Young and middle-aged scientific and technological innovation talents of Shenyang Science and Technology Bureau (RC170140), Liaoning Province Natural Science Foundation (20170540721), Basic research on the application of Industrial Development of Shenyang Science and Technology Bureau (18013027), Liaoning BaiQianWan Talents Program, and the Distinguished Professor Project of Liaoning province (20183532). We thank the Chinese Scholarship Council (20183058) for financial support. We thank Prof. Yohsuke Yamamoto and Dr. Rong Shang (Hiroshima University) for their help.

Supplementary data

Supplementary data to this article can be found online at https://doi.org/10.1016/j.tet.2xxxxxx

References and notes

1. V. Ntziachristos, J. Ripoll, R. Weissleder, Opt. Lett. 27 (2002) 333-335.
2. A. Becker, C. Hessenius, K. Licha, B. Ebert, U. Sukowski, W. Semmler, B. Wiedenmann, C. Grotzinger, Nat. Biotechnol. 19 (2001) 327-331.
3. R. Weissleder,V. Ntziachristos, Nat. Med. 9 (2003) 123-128.
4. F. Lv, B. Tang, E. Hao, Q. Liu, H. Wang, L. Jiao, Chem. Commun. 55 (2019) 1639-1642.
5. F. Ma, L. Zhou, C. Li, Y. Xie, Org. Lett. 21 (2019) 733-736.
6. Y. Ding, Y. Tang, W. Zhu, Y. Xie, Chem. Soc. Rev. 44 (2015) 1101-1112.
7. Q. Wang, X. Wei, C. Li, Y. Xie, Dyes Pigm. 148 (2018) 212-218.
8. Y. Ding, W. Zhu, Y. Xie, Chem. Rev. 117 (2017) 2203-2256.
9. X. Wei, L. Bu, H. Ågren, Y. Xie, Dye. Pigm. 136 (2017) 480-487.
10. C. Zhao, X. Zhang, K. Li, S. Zhu, Z. Guo, L. Zhang, F. Wang, Q. Fei, S. Luo, P. Shi, H. Tian, W. Zhu, J. Am. Chem. Soc. 137 (2015) 8490-8498.
11. A. Loudet. K. Burgess, Chem. Rev. 107 (2007) 4891-4932.
12. G. Ulrich, A. Harriman, R. Ziessel, Angew. Chem., Int. Ed. 47 (2008) 1184-1201.
13. A. Bessette, G. S. Hanan, Chem. Soc. Rev. 43 (2014) 3342-3405.
14. H. Lu, J. Mack, Y. Yang, Z. Shen, Chem. Soc. Rev. 43 (2014) 4778-4823.
15. T. Kowada, H. Maeda, K. Kikuchi, Chem. Soc. Rev. 44 (2015) 4953-4972.
16. H. Lu, S. Shimizu, J. Mack, Z. Shen, N. Kobayashi, Chem. Asian J. 6 (2011) 1026-1037.
17. S. O. McDonnell, M. J. Hall, L. T. Allen, A. Byrne, W. M. Gallagher, D. F. O'Shea, J. Am. Chem. Soc. 127 (2005) 16360-16361.
18. M.J. Hall, L.T. Allen, D. F. O'Shea, Org. Biomol. Chem. 4 (2006) 776-780.
19. R. Gresser, M. Hummert, H. Hartmann, K. Leo, M. Riede, Chem. Eur. J. 17 (2011) 2939-2947.
20. J. Killoran, L. Allen, J. Gallagher, W. Gallagher, D.F. O'Shea, Chem. Commun. (2002) 1862-1863.
21. J. Killoran, D.F. O'Shea, Chem. Commun. (2006) 1503-1505.
22. S.O. McDonnell, D.F. O'Shea, Org. Lett. 8 (2006) 3493-3496.
23. L. Jiao, Y. Wu, S. Wang, X. Hu, P. Zhang, C. Yu, K. Cong, Q. Meng, E. Hao, M.G.H. Vicente, J. Org. Chem. 79 (2014) 1830-1805.
24. X. Zhang, H. Yu, Y. Xiao, J. Org. Chem. 77 (2012) 669-673.
25. Q. Bellier, F. Dalier, E. Jeanneau, O. Maury, C. Andraud, New J. Chem. 36 (2012) 768-773.
26. K. Umezawa, Y. Nakamura, H. Makino, D. Citterio, K. Suzuki, J. Am. Chem. Soc. 130 (2008) 1550-1551.
27. S.G. Awuah, J. Polreis, V. Biradar, Y. You, Org. Lett. 13 (2011) 3884-3887.
28. Q. Y.W. Zhong, Z. Gong, J. Shao, J. Yao, Coord. Chem. Rev. 132 (2016) 22-40.
29. Y. Wu, C. Cheng, L. Jiao, C. Yu, S. Wang, Y. Wei, X. Mu, E. Hao, Org. Lett. 16 (2014) 748-751.
30. E. Heyer, P. Retailleau, R. Ziessel, Org. Lett. 16 (2014) 2330-2333.
31. S.O. McDonnell, D.F. O'Shea, Org. Lett. 8 (2006) 3493-3496.
32. K. Rurack, M. Kollmannsberger, J. Daub, Angew. Chem., Int. Ed. 40 (2001) 385-387.
33. Z. Diwu, C. Chen, C. Zhang, D.H. Klaubert, R.P. Haugland, Chem. Biol. 6(1999) 411-418.
34. C. Kue, S. Ng, S. Voon, A. Kamkaew, L. Chung, L. Kiew, H. Lee, Photochem. Photobiol. Sci. 17 (2018) 1691-1708.
35. X.D. Jiang, S. Li, B. Le Guennic, D. Jacquemin, D. Escudero, L. Xiao, Phys. Chem. Chem. Phys. 18 (2016) 32686-32690.
36. X.D. Jiang, J. Zhao, D. Xi, H. Yu, J. Guan, S. Li,C. Sun, L. Xiao, Chem. Eur. J. 21 (2015) 6079-6082.
37. X.-D. Jiang, J. Zhao, Q. Li, C. Sun, J. Guan, G. Sun, L. Xiao, Dyes Pigm. 125 (2016) 136-141.
38. X.-D. Jiang, J. Guan, J. zhao, B. Le Guennic, S. Li, D. Jacquemin, Z. Zhang, L. Xiao, Dyes Pigm. 136 (2017) 619-626.
39. T. Fang, X.D. Jiang, C. Sun, Q. Li, Sen. Actuators B 290 (2019) 551-557.
40. X.D. Jiang, J. Zhang, T. Furuyama, W. Zhao, Org. Lett. 14 (2012) 248-251.
41. A.F. Khlebnikov, M.S. Novikov, N.V. Rostovskii, Tetrahedron, (2019), DOI: 10.1016/j.tet.2019.03.040.
42. W. Zhao, E.M. Carreira, Angew. Chem., Int. Ed. 44 (2005) 1677-1679.
43. X.D. Jiang, T. Zhang, C. Sun, Y. Meng, L. Xiao, Chin. Chem. Lett. (2019) DOI: 10.1016/j.cclet.2019.02.016.
44. P. Shi, X.D. Jiang, R. Gao, Y. Dou, W. Zhao, Chin.Chem. Lett. 26 (2015) 834-838.
45. L. Fabbrizzi, A. Poggi, Chem. Soc. Rev. 24 (1995) 197-202.
46. B. Valeur, J.R. Lakowicz (Ed.), Topics in Fluorescence Spectroscopy, Probe Design and Chemical Sensing, 4 Plenum, New York, 1994, p. 21.

47. M.J. Frisch, G.W. Trucks, H.B. Schlegel, G.E. Scuseria, M.A. Robb, J.R. Cheeseman, G. Scalmani, V. Barone, B. Mennucci, G. A. Petersson, H. Nakatsuji, M. Caricato, X. Li, H.P. Hratchian, A.F. Izmaylov, J. Bloino, G. Zheng, J.L. Sonnenberg, M. Hada, M. Ehara, K. Toyota, R. Fukuda, J. Hasegawa, M. Ishida, T. Nakajima, Y. Honda, O. Kitao, H. Nakai, T. Vreven, J. A., Jr. Montgomery, J.E. Peralta, F. Ogliaro, M. Bearpark, J.J. Heyd, E. Brothers, K.N. Kudin, V.N. Staroverov, R. Kobayashi, J. Normand, K. Raghavachari, A. Rendell, J.C. Burant, S.S. Iyengar, J. Tomasi, M. Cossi, N. Rega, J. M. Millam, M. Klene, J.E. Knox, J.B. Cross, V. Bakken, C. Adamo, J. Jaramillo, R. Gomperts, R.E. Stratmann, O. Yazyev, A. J. Austin, R. Cammi, C. Pomelli, J.W. Ochterski, R.L. Martin, K. Morokuma, V.G. Zakrzewski, G.A. Voth, P. Salvador, J.J. Dannenberg, S. Dapprich, A.D. Daniels, Ö. Farkas, J.B. Foresman, J.V. Ortiz, J. Cioslowski and D.J. Fox, Gaussian 09W, revision A.1; Gaussian Inc.: Wallingford, CT, 2009.
48. L. Huang, X. Cui, B. Therrien, J. Zhao, Chem.-Eur. J. 19 (2013) 17472-17482.
49. J. Zhang, Q. Wang, Z. Guo, S. Zhang, C. Yan, H. Tian, W. Zhu, Adv. Funct. Mater. 29 (2019) 1808153.
50. A. Gorman, J. Killoran, C. O'Shea, T. Kenna, W.M. Gallagher, D.F. O'Shea, J. Am. Chem. Soc. 126 (2004) 10619-10631.

1) Morpholino-containing aza-BODIPYs at 3,5-positions were synthesized.
2) Aza-BODIPY **1** with the morpholino group as a pH-sensitive functionality could be used to be a pH probe.
3) The singlet oxygen generation of PS **2** with the dibromo groups at 2,6-positions was more effective than that of the parent dye **1**.